Journal of Geodetic Science

• 1(2) • 2011 • 158-169 DOI: 10.2478/v10156-010-0019-y •

Positioning and Position Error of Petroleum Wells

Research Article

Tony Gjerde[1], Jo Eidsvik[2]*, Erik Nyrnes[3], Bjørn T. Bruun[3]

1 Scandpower AS, 2027 Kjeller, Norway
2 Department of Mathematical Sciences, 7491 Trondheim, NTNU, Norway
3 Statoil Research Center, Rotvoll, 7000 Trondheim, Norway

Abstract:

We present a new model for the estimation of positional uncertainty of petroleum wells. The model uses a heavy tailed normal inverse Gaussian distribution for the errors in Earth's magnetic field reference values. These references are required for calculating the position of a well using magnetic directional surveying. The results show that the normal inverse Gaussian distribution gives a more realistic fit to the Earth's magnetic field reference values than the normal distribution, which is the current state of art. Errors in surveying sensors and reference errors are propagated along the well path to obtain the positioning uncertainty. The positional uncertainty is important for the probability of collisions between wells and for drilling accurate relief wells when an eventual collision has resulted in a blow-out situation. We compare results of the normal model used in the petroleum industry with our proposed model. The comparison is made for anti-collision calculations between drilled wells and a planned well. The results indicate a higher risk of collisions for certain well geometries when using the normal distribution, while a collision is avoided in the normal inverse Gaussian situation. We find clear differences between an approximate normal test and a Monte Carlo test.

Keywords:

anti-collision • directional drilling • error propagation • heavy tails • magnetic surveying • normal inverse Gaussian distribution

© *Versita Warsaw and Springer-Verlag Berlin Heidelberg.*

Received 28 January 2011; accepted 13 March 2011

1. Introduction

While early petroleum wells were vertical, current ones are steered using directional drilling techniques. This entails careful planning of the drilling path in an existing geographic model of the petroleum reservoir zone, and using measurement instruments while drilling to maintain operation control. Directional drilling has several advantages. For instance, wells can be drilled from a platform to several different reservoir zones, well plans can go around existing installations or difficult geologic formations, sidetracks from existing wells can be constructed, and horizontal wells in a reservoir zone can improve production. A real-time operation with multilateral wells significantly improved production at the Norwegian Troll field (Skarsbø and Ernesti, 2006). The gas from this field is produced from about 100 wells, and the total length of wellbore is more than 350 km. Within such settings it is important to avoid collisions with existing wells (Williamson, 1998), while still aiming for the best trajectory for optimal reservoir production. The worst scenario in the petroleum industry is a blow-out, caused either by a collision between two wells or improper well control. The accident in the Gulf of Mexico in 2010 has resulted in a sharper focus on the planning and drilling of accurate relief wells, which is vital for controlling and killing blow-out situations.

Measurement While Drilling (MWD) technology allows us to calculate the position of the well path in real-time during drilling operation. The instruments are mounted behind the drill bit, and the measurements are transferred to the surface in real-time for every well stand (30m). Amongst the most important data are

*E-mail: joeid@math.ntnu.no, phone: 4773590153, fax: 4773593524

VERSITA

Brought to you by | Universitetsbiblioteket I Trondheim NTNU Universitetsbiblioteket
Authenticated
Download Date | 10/7/19 3:25 PM

accelerometer and magnetometer measurements of the Earth's gravitational and magnetic fields, which are used to calculate the direction of the wellbore at each stand. In order to compute the position of the well, the along-hole distance is also required. Gyroscopic sensors (Noureldin et al., 2004) or seismic techniques (Rector and Marion, 1991) can also be used for positioning wells, but magnetic MWD instruments are the most common.

Positioning and uncertainty estimation in directional drilling have been studied by Wolff and de Wardt (1981) and Williamson (2000). They develop error models for the instrument measurements and the Earth's magnetic field reference values. It is by now common practice to propagate these error terms, using normal distributions, to obtain the position covariance. The model presented in Williamson (2000) extends the model proposed in Wolff and de Wardt (1981), splitting error contributions into global errors (constant for the entire survey), section specific errors (constant for a drilling section) and random error (changing between every drilling stand). The Williamson model has been accepted as an industry standard (http:// copsegrove. com/ ISCWSA.aspx). One caveat with the current standard is that it does not account for the heavy tailed nature of the magnetic reference values. For geomagnetic declination data we even observe some skewness, in addition to very heavy tails. The geodetic techniques would benefit from incorporating these error structures. In fact, the current methods for detecting gross errors in magnetic MWD directional surveys remove far too many position estimates, compared with the expected level under a normal assumption for the errors (Nyrnes, 2006).

In the current paper we embed the Williamson model into a more general framework, including the possibility of heavy tailed and skewed distributions for the Earth's magnetic field reference values. The idea of using heavy tailed distributions, such as contaminated normal distributions to include the impact of gross errors, goes back to the work done by Tukey (1960). Here, we use the Normal Inverse Gaussian (NIG) distribution (Barndorff-Nielsen, 1997), which is a flexible model for introducing heavy tails and skewness in this context. It enters naturally as a mixture over different normal distributions, and we will utilize this to simplify the computations. We show how the NIG distribution gives a more realistic error description for the magnetic field reference data acquired at geomagnetic observatories. Alternative distributions could also be useful, for instance the skew Student's t-distribution (Azzalini and Capitanio, 2003) or suitable generalizations (Genton, 2004).

The paper is organized as follows: Section 2.1 describes the deterministic relations used in magnetic MWD directional surveying, Section 2.2 presents the methods for positioning in both normal and NIG models, and Section 2.3 outlines anti-collision calculations as a relevant application. In Section 3 we show results for well positioning and anti-collision calculations.

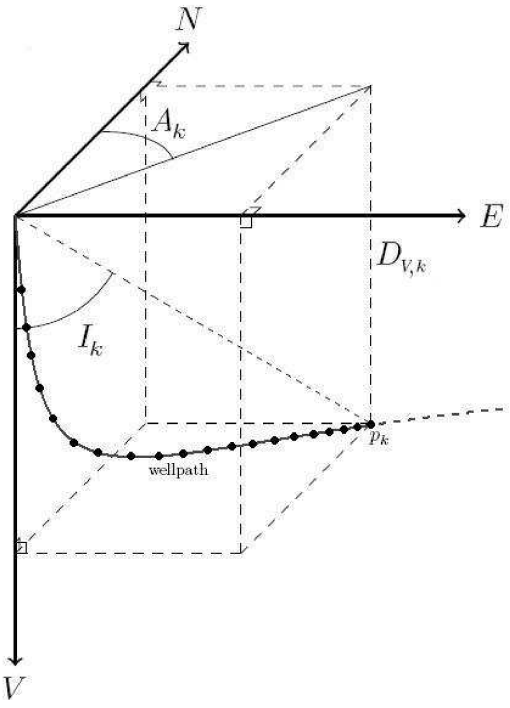

Figure 1. Illustration of well positioning. The coordinate system is north (N), east (E) and vertical depth (D_V). The position p_k is estimated at each stand (30m) of the well path. The inclination I is the angle between the vertical and the lateral coordinate. The azimuth A is the angle between the two lateral coordinates.

2. Experimental Procedures

2.1. Magnetic directional surveying

A drilling operation starts at the surface or the sea bottom and ends at a reservoir typically after a few kilometers. The operation is usually split into several drilling sections, where each section uses a different size of drill bit. We will consider the situation where a directional MWD survey is performed in discrete points along the well path with an interval of 30 m. We first describe the accelerometer and magnetometer measurements acquired at one survey point. Next, we show how these data are combined to obtain the geographic position in north (N), east (E) and vertical depth (D_V), see Figure 1.

The sensor constellation of an MWD magnetic directional surveying instrument consists of three accelerometers and three magnetometers. Based on the measurements from these sensors the azimuth and inclination angles at the survey points can be computed. By also measuring the depth (D) along the arc of the well path, and using magnetic field reference values, the position $\boldsymbol{p} = (N, E, D_V)$ along the well path can be calculated. The measured depth should not be confused with the vertical depth

Brought to you by | Universitetsbiblioteket I Trondheim NTNU Universitetsbiblioteket
Authenticated
Download Date | 10/7/19 3:25 PM

D_V. See Figure 1. While the Earth's gravity field is quite stable, the Earth's magnetic field is more unstable. It is a common practice to divide the Earth's magnetic field observed at the magnetic sensors into three different magnetic fields: The main field, the crustal field and the external field, see e.g. Merrill (1983). The external field is the most unpredictable part, because of high-frequent variations of relatively large magnitude. These variations can be observed at stationary geomagnetic observatories. A magnetic field reference component that is always required for positioning is the magnetic declination angle. The declination is defined as the deviation between geographic and magnetic north.

The accelerometers measure orthogonal components of the gravity field; the along-hole component G_z, and the two cross-axial components G_x and G_y. The inclination angle I is given by

$$I = I(G_x, G_y, G_z) = \operatorname{atan}\left(\frac{\sqrt{G_x^2 + G_y^2}}{G_z}\right). \qquad (1)$$

The error propagation models presented in the next section use a total gravity reference value of $G = 9.8\ m/s^2$.

Magnetometer measurements consist of the three orthogonal components of the Earth's magnetic field; B_x, B_y and B_z, where B_z is aligned along the well path. The magnetic azimuth angle A_m is commonly calculated by (Ekseth, 1998):

$$A_m = \operatorname{atan}\left(\frac{(G_x B_y - G_y B_x)\sqrt{G_x^2 + G_y^2 + G_z^2}}{B_z(G_x^2 + G_y^2) - G_z(G_x B_x + G_y B_y)}\right). \qquad (2)$$

The total magnetic field intensity B, magnetic dip angle θ, and declination δ is an equivalent parameterization of the Earth's magnetic field. These magnetic field parameters vary across the Earth. For the North Sea, which is of most relevance for us, the total magnetic field intensity B is approximately 51000 nT. Similarly, approximate values for the magnetic declination $\delta = 1^o$ and dip angle $\theta = 75^0$. The geometric azimuth A is obtained by

$$A = A(G_x, G_y, G_z, B_x, B_y, B_z, \delta) = A_m + \delta, \qquad (3)$$

where we see that the magnetic declination angle δ is a required correction to equation (2).

In some cases the along-hole magnetometer measurement B_z is affected by magnetic interference from components in the drillstring and down-hole drilling equipment. In such situations it is a common procedure to ignore the real B_z component, and instead apply an approximation of the B_z component, calculated from the local reference values for the total magnetic field strength B and dip angle θ. The main drawback of this method is that the azimuth uncertainty increases considerably as the well approaches horizontal east-west directions, see e.g. Bang et al. (2009).

The position of the drillbit at a survey point of interest is obtained by summing up all the relative position differences from the drilling operation starts to the survey point. The most common method for position calculation is the minimum curvature (Thorogood and Sawaryn, 2005). Let $\boldsymbol{p}_{k-1}$ be the north, east and vertical depth position at the previous stand $k-1$, and let further I_{k-1}, I_k and A_{k-1}, A_k denote the two consecutive inclination and azimuth angles computed at the last two stands $k-1, k$. Thorogood and Sawaryn (2005) derive the following formula:

$$\boldsymbol{p}_k = \boldsymbol{p}_{k-1} + \frac{(D_k - D_{k-1})h_k}{2}\boldsymbol{v}_{k-1,k}, \qquad (4)$$

where the last vector is a function of inclinations and azimuths;

$$\boldsymbol{v}_{k-1,k} = \begin{bmatrix} \sin I_{k-1}\cos A_{k-1} + \sin I_k \cos A_k \\ \sin I_{k-1}\sin A_{k-1} + \sin I_k \sin A_k \\ \cos I_{k-1} + \cos I_k \end{bmatrix}. \qquad (5)$$

Further, the function $h_k = h(I_{k-1}, I_k, A_{k-1}, A_k) \approx 1$ is a measure of the change in inclination and azimuth angles along the well path.

2.2. Statistical model for position uncertainty

We now outline a statistical model for positioning, as an extension to the deterministic formulas in Section 2.1. First, the main sources of error are described along with their assumed distributions. Next, error propagation is used to derive the position distribution. This is directly applicable for the case with only normally distributed errors, and is then extended to the case of NIG distributed errors for the Earth's magnetic field reference values.

2.2.1. *Error models for MWD magnetic surveying*

We specify 21 error sources that are relevant for assessing the position uncertainty of a well (Williamson, 2000). For the sensor errors we use normal distributions, while the magnetic reference values are modelled by heavy tailed NIG distributions. This choice is justified empirically using geomagnetic observatory data at the end of this subsection.

Table 1 summarizes the error sources, their assumed standard deviation and units, and the propagation mode. These assumptions for the errors are taken from Williamson (2000). A global propagation mode (G) entails that the error is constant for the entire drilling operation, section specific propagation mode (S) means that the error is constant within a drilling section, while the random propagation mode (R) uses a new random error at every stand in each section. Note that the G and S mode corresponds to errors that induce bias since they are constant over several stands. The G and S error modes were also discussed by Wolff and de Wardt (1981).

Brought to you by | Universitetsbiblioteket I Trondheim NTNU Universitetsbiblioteket
Authenticated
Download Date | 10/7/19 3:25 PM

Table 1. Overview of the different error sources. All the error sources are assumed independent. The error sources affect MWD surveys in different propagation modes. (R: Random, S: Systematic, G: Global). The superscript star notation means that B_z is not always useful. When this takes place, one uses the reference magnetic dip and strength denoted by superscript plus.

Error number	Description	Standard deviation	Mode
1-3	G_x, G_y, G_z bias	0.0039 m/s^2	S
4-6	G_x, G_y, G_z scale	0.0005	S
7-9*	B_x, B_y, B_z bias	70 nT	S
10-12*	B_x, B_y, B_z scale	0.0016	S
13	Depth reference	0.35 m	R
14	Depth scale factor	$6 \cdot 10^{-4}$	S
15	Depth stretch type	$2.5 \cdot 10^{-7}$ m^{-1}	G
16	Inclination, Sag	0.2°	S
17	Azimuth, drill string	150 nT	S
18	Azimuth, B_H dependent	5000° nT	G
19	Magnetic declination (δ)	0.36°	G
20$^+$	Magnetic dip (θ)	0.2°	G
21$^+$	Magnetic strength (B)	150 nT	G

For the accelerometers and magnetometers we assume that the sensor readings are given by

$$u = \mu_u + \epsilon_{b,u} + \mu_u \epsilon_{s,u}, \qquad u = G_x, G_y, G_z, B_x, B_y, B_z, \quad (6)$$

where μ_u is the fixed, unknown value of the accelerometer or magnetometer components, the error $\epsilon_{b,u}$ is referred to as the bias error in the instrument, while the error $\epsilon_{s,u}$ is the scale factor error in the instrument. All errors $\epsilon_{b,u}$ and $\epsilon_{s,u}$ are assumed to have propagation mode S. Since we have three gravitation measurements and three magnetic measurements, all with a bias and scale factor, these errors constitute the $\epsilon_1, \ldots, \epsilon_{12}$ in Table 1, where $\epsilon_1 = \epsilon_{b,G_x}$, $\epsilon_2 = \epsilon_{b,G_y}$, etc.

The next error type is associated with the along-hole depth readings D given by

$$D = \mu_D + \epsilon_{13} + \mu_D \cdot \epsilon_{14} + \mu_D \cdot \mu_{D_V} \cdot \epsilon_{15}, \quad (7)$$

where μ_D is the true along-hole depth and μ_{D_V} is the vertical depth. The modes of the three errors are given in Table 1. The major contributors to errors in the inclination and magnetic azimuth are deformation of the drilling equipment due to gravity (sag) and the magnetization of the drill-string. For inclination

$$I = \mu_I(\mu_{G_x}, \mu_{G_y}, \mu_{G_z}) + \sin(\mu_I)\epsilon_{16}, \quad (8)$$

where μ_I is the functional relationship in equation (1). For azimuth

$$A = \mu_A + \frac{\sin\mu_I \sin\mu_{A_m}}{\mu_B \cos\mu_\theta}\epsilon_{17} + \frac{1}{\mu_B \cos\mu_\theta}\epsilon_{18} + \epsilon_{19}, \quad (9)$$

where $\mu_A = \mu_A(\mu_{G_x}, \mu_{G_y}, \mu_{G_z}, \mu_{B_x}, \mu_{B_y}, \mu_{B_z}, \mu_\delta)$ is the functional relationship in equation (3), while ϵ_{17} and ϵ_{18} are drillstring and down-hole magnetism errors. The error ϵ_{19} is related to the bias in magnetic declination δ. The error terms ϵ_{20} and ϵ_{21} are biases in the reference values for magnetic dip and field strength. Like the declination error ϵ_{19} they have a propagation mode G, since a constant reference value is used throughout the drilling operation. Recall that the error term ϵ_{19} is always required, while errors in magnetic dip angle and magnetic field strength (ϵ_{20} and ϵ_{21}) are only used if the B_z component cannot be trusted during the MWD operation.

Williamson (2000) used a normal distribution for all error sources $\epsilon_1, \ldots, \epsilon_{21}$, but pointed out that the magnetic reference errors seem to have heavier tails than a normal distribution. We use a normal distribution with zero mean and standard deviations given in Table 1 for the sensor errors ϵ_1-ϵ_{18}. For the magnetic reference values ϵ_{19}-ϵ_{21} we use a heavy tailed NIG distribution. The NIG density function for $x \in \mathbf{R}$ is

$$f(x) = \frac{\alpha\rho K_1\left(\alpha\sqrt{\rho^2 + (x-\mu)^2}\right)}{\pi\sqrt{\rho^2 + (x-\mu)^2}} \cdot \exp\left\{\rho\sqrt{\alpha^2 - \beta^2} + \beta(x-\mu)\right\}, \quad (10)$$

where μ, ρ, α and β are model parameters, and $K_1(\cdot)$ is the modified Bessel function of the third kind and index 1 (Barndorff-Nielsen, 1997). The NIG distribution can be regarded as a mean-variance mixture distribution of the normal via the following two-step scheme:

i) Let z be Inverse Gaussian (IG) distributed, $z \sim IG(\rho, \gamma)$, $\gamma = \sqrt{\alpha^2 - \beta^2}$, i.e. for $z > 0$,

$$f(z) = \frac{1}{\sqrt{2\pi z^3}}\rho \exp\left\{\rho\gamma - \frac{1}{2}\left(\frac{\rho^2}{z} + \gamma^2 z\right)\right\}. \quad (11)$$

ii) Let $x|z$ be normal (N) distributed, i.e. $f(x|z) \sim N(\mu + \beta z, z)$. Then the joint density is $f(x, z) = f(x|z)f(z)$ and the marginal distribution $f(x) = \int f(x, z)dz$, derived by marginalization over z, is the NIG density. Intuitively this says that for each z value, the x variate is normal, but we are not sure which z to use, and we integrate over many z instead of conditioning on one in particular. The resulting (marginal) distribution for x has heavy tails and skewness as a result of the weighting with different $f(z)$. The more common Student's t-distribution can be derived in a similar manner using a conditional formulation and marginalization, but with different $f(x|z)$ and $f(z)$ distributions, giving a variance mixture only. Note that the Student's t-distribution does not allow for skewness. The generalization known as the skew-t distribution (Azzalini and Capitanio, 2003) has the same number of parameters as the NIG distribution, but gives much less flexibility in the skewness and tail behaviour.

In Figure 2 we show the histograms of magnetic declination (left, top), dip (left, middle) and strength (left, below) readings made

VERSITA

Brought to you by | Universitetsbiblioteket I Trondheim NTNU Universitetsbiblioteket
Authenticated
Download Date | 10/7/19 3:25 PM

in 2001 at the geomagnetic observatory in Tromsø, Norway. The data consists of one year of registration, sampled every minute. This gives about 500000 measurements in total. We processed the data by removing a time trend, and scaling the residuals to have a variance equal to that given by Williamson (2000) as shown in Table 1. In the middle and right column of Figure 2 we display quantile-quantile (QQ) plots of the data using normal and NIG distributions. If a distribution is appropriate, the associated QQ plot should be close to the straight line. The middle column of Figure 2 shows QQ plots of a normal distribution fitted to the data. Apparently, the tails are far too heavy to be modeled by a normal distribution. In the right column of Figure 2 we show the QQ plots for a NIG fit to the data. This gives a much better representation of the data, justifying that the magnetic reference values are more realistically modeled by a NIG distribution. The normal distribution is easy to fit by simply taking the empirical mean and standard deviation of the data. The fitted NIG parameters are obtained by setting the centrality parameter $\mu = 0$, and tuning α, β and ρ to match every 10th empirical percentile in a least squares sense. For magnetic declination this gives: $\mu_\delta = 0$, $\rho_\delta = 0.003$, $\alpha_\delta = 58$, and $\beta_\delta = 14$, for magnetic dip $\mu_\theta = 0$, $\rho_\theta = 0.001$, $\alpha_\theta = 100$, and $\beta_\theta = 40$, and for magnetic field strength $\mu_\theta = 0$, $\rho_\theta = 32$, $\alpha_\theta = 0.002$, and $\beta_\theta = 0.0005$. We also experimented with $\mu \neq 0$, but got results very close to 0 and a similar fit to the data. An alternative estimation procedure is the Expectation Maximization (EM) algorithm (Karlis, 2000), which is an iterative method for computing the maximum likelihood estimates. For our data we struggled with the convergence in this approach, and we preferred the more robust percentile fitting. The development of a robust EM algorithm for this situation is a topic for future work.

2.2.2. Positioning with normal errors

The error sources defined in the previous section propagate in the physical relations for positioning using MWD directional drilling. We now consider error propagation for positioning in the case of normally distributed errors.

The north, east and vertical depth position $\boldsymbol{p}_k$ at stand k is a random variable. Its probability distribution depends on the distribution of the position at the previous stand $k-1$ and the distribution of azimuth, inclination and depth calculated from sensor readings at stand $k-1$ and k along with magnetic reference values. Equation (4) and (5) summarize this, and can be rephrased as

$$\boldsymbol{p}_k = \boldsymbol{p}_0 + \sum_{l=1}^{k} \frac{(D_l - D_{l-1})h_k}{2} \boldsymbol{v}_{l-1,l} \tag{12}$$

where D_0, I_0, A_0 and the initial position $\boldsymbol{p}_0$ are fixed from initial drilling conditions. When we linearize the nonlinear expression (12), and assume that all error sources are normally distributed, the north, east and vertical depth positions $\boldsymbol{p}_k$ are also normally distributed;

$$\boldsymbol{p}_k \sim N(\hat{\boldsymbol{p}}_k, \boldsymbol{\Omega}_k), \qquad k = 1, 2, \ldots, \tag{13}$$

with mean position vector $\hat{\boldsymbol{p}}_k$ and a 3×3 covariance matrix $\boldsymbol{\Omega}_k$. The mean position is estimated by plugging in the sensor readings directly for all μ in Section 2.1. For the covariance we use linearized versions of the physical relations for positioning.

The propagation modes (R, S or G) of the errors are important for the covariance calculation, since it affects the weights in the error propagation formula used to obtain $\boldsymbol{\Omega}_k$. For instance, the error ϵ_{16} in inclination I_l depends on the section specific (S) errors in the accelerometers. These errors are identical for I_l and I_{l+1} if the two stands l and $l+1$ are within the same section, otherwise they are different. The accelerometer error propagates according to

$$\mathrm{Var}(I_l) \approx \sum_{u \in x,y,z} \frac{dI_l}{dG_{u,l}} \mathrm{Var}(G_{u,l}) \frac{dI_l}{dG_{u,l}}, \tag{14}$$

where the derivatives can be calculated by equation (1), and the expression is evaluated at the $G_{x,l}$, $G_{y,l}$ and $G_{z,l}$ readings at stand l. There are no cross-terms of derivatives or covariances in this formula, since the error sources are assumed independent. We can treat the propagation modes R, S and G separately and the 3×3 covariance is then

$$\boldsymbol{\Omega}_k = \sum_R \boldsymbol{\Omega}_{R,k} + \sum_S \boldsymbol{\Omega}_{S,k} + \sum_G \boldsymbol{\Omega}_{G,k}. \tag{15}$$

For a section specific (S) error source ϵ with $\mathrm{Var}(\epsilon) = \sigma_S^2$ we get

$$\begin{aligned} \boldsymbol{\Omega}_{S,L,k} &= \sum_{l=1}^{L-1} \sum_{i=1}^{n_l} \boldsymbol{R}_{l,i,i+1} \boldsymbol{w}_{S,l,i} \sigma_S^2 \boldsymbol{w}'_{S,l,i} \boldsymbol{R}'_{l,i,i+1} \\ &+ \boldsymbol{q} \sigma_S^2 \boldsymbol{q}', \\ \boldsymbol{q} &= \boldsymbol{Q}_{L,k,k} \boldsymbol{w}_{S,L,k} + \sum_{i=1}^{k-1} \boldsymbol{R}_{L,i,i+1} \boldsymbol{w}_{S,L,i}, \\ \boldsymbol{R}_{l,i,i+1} &= \boldsymbol{Q}_{l,i,i} + \boldsymbol{Q}_{l,i+1,i}, \end{aligned} \tag{16}$$

where $\boldsymbol{Q}_{l,i,i}$ are partial derivatives of north, east and vertical depth position in equation (12), taken with respect to the inclination, azimuth and along-hole depth, i.e. $\frac{d\boldsymbol{p}_l}{dA_i, dI_i, dD_i}$, $i, l = 1, \ldots, k$. Further, $\boldsymbol{w}_{S,l,i}$ are partial derivatives of inclination, azimuth and depth, taken with respect to a section specific error, i.e. $\frac{dA_l, dI_l, dD_l}{d\epsilon}$. Finally, the index l is over the $L-1$ first sections, while i is an index for the stands in the current section L, where k is the last stand. These derivatives are further explained in Gjerde (2008).

If the B_Z measurement is not reliable, the errors ϵ_9 and ϵ_{12} in Table 1 are no longer relevant. Instead the magnetic dip angle θ and field strength B take part in the positioning formula. Consequently, the errors ϵ_{20} and ϵ_{21} are required in the propagation formulas.

Brought to you by | Universitetsbiblioteket I Trondheim NTNU Universitetsbiblioteket
Authenticated
Download Date | 10/7/19 3:25 PM

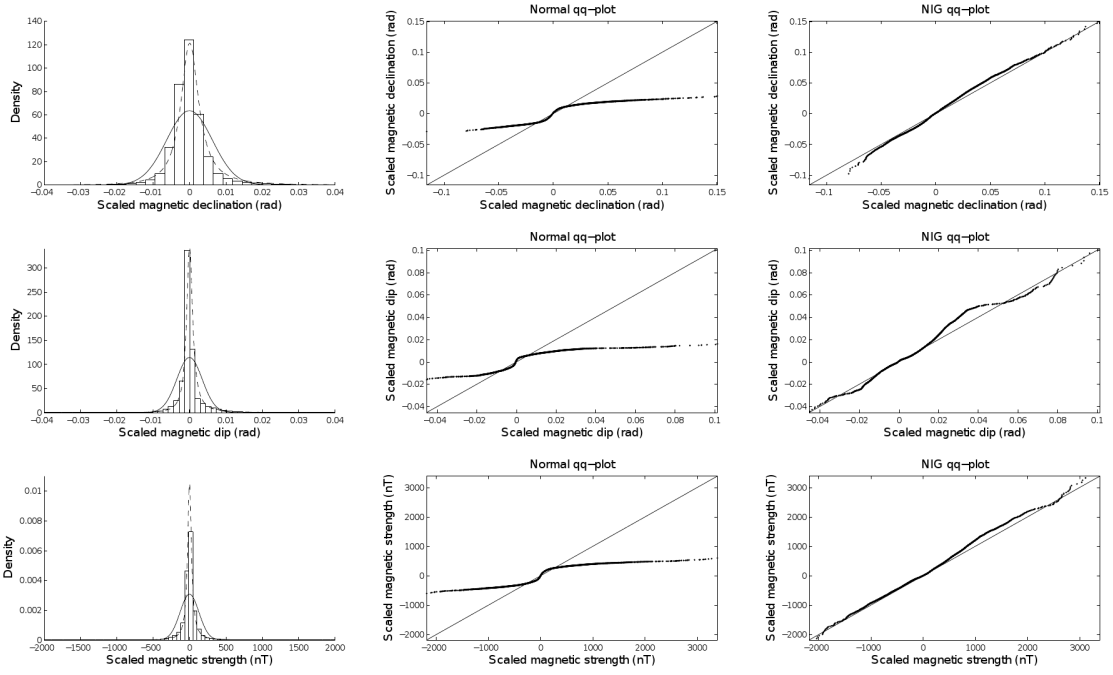

Figure 2. Data analysis of magnetic reference field observations at the geomagnetic observatory in Tromsø, Norway, in the year 2001. Magnetic declination (top), magnetic dip (middle) and magnetic strength (bottom). Left: Histogram with fitted normal (solid) and NIG (dashed) distribution. Middle: QQ plots using the normal distribution. Right: QQ plots using the NIG distribution.

2.2.3. *Positioning with NIG errors*

Recall that the magnetic declination reference δ has an associated error ϵ_{19}. We now present a model for position uncertainty assuming the NIG distribution for this declination error. The other error sources are still assumed normal.

The NIG distribution is closed under linearity, with certain regularity conditions of common α and β, see e.g. Barndorff-Nielsen (1997), Karlis (2000) and Øigård et al. (2005), but in our case these do not apply because of the linearization. Our approach for including a NIG distributed error in the positioning distribution for $\boldsymbol{p}_k$ is based on the conditional formulation of the NIG distribution. By defining $\epsilon_{19} \sim NIG(\mu, \rho, \alpha, \beta)$ and using equation (11) we get

$$\{\epsilon_{19}|z\} \sim N(\mu + \beta z, z), \qquad z \sim IG(\rho, \gamma), \tag{17}$$

where $\gamma = \sqrt{\alpha^2 - \beta^2}$.

When we condition on z, the methodology developed in Section 2.2.2 holds with a normal distribution for the position $\boldsymbol{p}_k$. After marginalization, the distribution for $\boldsymbol{p}_k$ becomes a mixture distribution. The mixture is no longer NIG distributed, since the normal $\boldsymbol{p}_k|z$ is not in the required form, see point ii) below equation (11). The marginal distribution for $\boldsymbol{p}_k$, $k = 1, \ldots$, is defined as

$$f(\boldsymbol{p}_k) = \int f(\boldsymbol{p}_k|z) f(z) \mathrm{d}z \tag{18}$$

where $f(\boldsymbol{p}_k|z) = N(\hat{\boldsymbol{p}}_k(z), \boldsymbol{\Omega}_k(z))$ is calculated using equation (13) for a fixed z, and with $f(z)$ defined in equation (17). The mean position $\hat{\boldsymbol{p}}_k(z)$ is calcuated using relations for positioning, but now using the declination bias error $\epsilon_{19}|z \sim N(\mu + \beta z, z)$. The covariance $\boldsymbol{\Omega}_{G,k} = \boldsymbol{\Omega}_{G,k}(z)$ in equation (15) is evaluated at a new value for declination angle, but the random and section specific covariance parts $\boldsymbol{\Omega}_{R,k}$ and $\boldsymbol{\Omega}_{S,k}$ remain the same. The integral in equation (18) is approximated numerically by

$$f(\boldsymbol{p}_k) \approx \sum_{z_i \in F} f(\boldsymbol{p}_k|z_i) f(z_i), \qquad \sum_{z_i \in F} f(z_i) = 1, \tag{19}$$

where $f(z_i)$ is a numerical discretization of the IG density over a regular grid F covering the non-negligible probability mass.

If B_z is not reliable, the magnetic dip angle θ and field intensity B are involved in the calculation of position $\boldsymbol{p}_k$. Thus, there are three reference values and three associated NIG error components in the model: the errors ϵ_{19}, ϵ_{20}, and ϵ_{21}. This entails that equation (18) involves a three dimensional integral. The integral is approximated numerically by a sum over a three dimensional grid in equation (19).

VERSITA

Brought to you by | Universitetsbiblioteket I Trondheim NTNU Universitetsbiblioteket
Authenticated
Download Date | 10/7/19 3:25 PM

2.3. Anti-collision calculations

One of the worst scenarios in a drilling operation is collision with other wells. To reduce the risk of such an event, petroleum companies perform anti-collision calculations for every planned well (Williamson, 1998). Based on these anti-collision calculations, the proposed well plan is either acknowledged and drilled, or re-planned such that it fulfills the requirements. This decision is made using a hypothesis test of which the test statistic is based on the calculated distance between two wells. The distance is defined as the shortest center-to-center distance between the planned well (reference well) and the other earlier drilled wells (offset wells). The null hypotheses is a well collision, and a well plan is realized only if this hypothesis is rejected for every stand of the well path. Alternative decision rules are certainly possible here, for instance a criterion based on multiple testing or integrated risk, but we have chosen to focus on the above criterion, which forms the current state-of-the-art.

The anti-collision calculations are performed with respect to the 'closest' point in an offset well. The closest point is determined using a '3D closest approach' based on the minimal Euclidean distance between a scanning point in the reference well and any point in the offset wells. The hypothesis test is formulated in terms of the expected closest center-to-center distance.

Let $\boldsymbol{p}$ be the position coordinates at one scanning point in the reference well, and $\boldsymbol{q}$ the 3D closest point in any of the offset wells. The index k is ignored here. We assume that these positions are independent. In the first part below we also assume a normal distribution;

$$\boldsymbol{p} \sim N(\boldsymbol{\mu}_p, \boldsymbol{\Omega}), \qquad \boldsymbol{q} \sim N(\boldsymbol{\mu}_q, \boldsymbol{\Sigma}), \tag{20}$$

where the means $\boldsymbol{\mu}_p = \hat{\boldsymbol{p}}$ and $\boldsymbol{\mu}_q = \hat{\boldsymbol{q}}$ are found using the deterministic methods in Section 2.1. Further, $\boldsymbol{\Sigma}$ and $\boldsymbol{\Omega}$ are the associated position covariance matrices. The center-to-center distance is $d = \sqrt{\boldsymbol{r}^T \boldsymbol{r}}$, $\boldsymbol{r} = \boldsymbol{p} - \boldsymbol{q}$. We perform hypothesis testing on the expected center-to-center distance μ_d. Let H_0 denote a well collision and H_1 no well collision. This entails

$$H_0: \quad \mu_d \leq \mu_{d,0}, \qquad H_1: \quad \mu_d > \mu_{d,0}, \tag{21}$$

where $\mu_{d,0}$ is the sum of the borehole radii of the two wells.

2.3.1. Normal approximation test

We first describe a test based on an approximate normal distribution for the center-to-center distance d. Note that distance vector $\boldsymbol{r}$ is normal when all error sources are assumed normal, but the distance d is not normal. An approximate normal distribution for the center-to-center distance is obtained by linearization of $d = \sqrt{\boldsymbol{r}^T \boldsymbol{r}}$ to obtain

$$d \approx N(\mu_d, \sigma_d^2), \qquad \sigma_d^2 = \frac{1}{\hat{\boldsymbol{r}}^T \hat{\boldsymbol{r}}} \hat{\boldsymbol{r}}^T (\boldsymbol{\Omega} + \boldsymbol{\Sigma}) \hat{\boldsymbol{r}}, \tag{22}$$

where $\hat{r} = \hat{p} - \hat{q}$. Under H_0 the center-to-center distance $d \approx N(\mu_{0,d}, \sigma_d^2)$. We reject H_0 on significance level α if the observed distance d^{obs} is such that $\frac{d^{\text{obs}} - \mu_{0,d}}{\hat{\sigma}_d} > \kappa_\alpha$, where κ_α is the $100(1-\alpha)$ percentile of the standard normal distribution. With $\alpha = \frac{1}{500} = 0.002$, $\kappa_{\alpha,1} = 2.878$. Instead of using a fixed level, one could consider the p-value, which is the smallest significance level α for which a hypothesis is rejected. If the p-value is small, we reject H_0. In the petroleum industry the separation factor defined by $\omega = \frac{d^{\text{obs}} - \mu_{d,0}}{k_{\alpha,1} \hat{\sigma}_d}$ is also commonly used. Then H_0 is rejected if $\omega > 1$. A rejection of H_0 entails that the distance between wells is sufficiently large. If a rejection occurs at every stand in the well, a well plan can be realized.

The normal assumption on the distribution of the center-to-center distance d may not be reliable for short distances. Short distances provide the highest risk in drilling situations, so it is of interest to avoid using this normal approximation for more reliable anti-collision calculations. Further, the normal distribution is defined on $(-\infty, \infty)$, while the distance d takes non-negative values only.

2.3.2. Monte Carlo tests

Monte Carlo tests allow any distribution for the test statistic. For the NIG error situation we use a reference well position $\boldsymbol{p} \sim f(\boldsymbol{p})$, which is defined by equation (19). The offset well position $\boldsymbol{q} \sim N(\boldsymbol{\mu}_q, \boldsymbol{\Omega})$. This normal assumption can be justified since the offset well is usually monitored by an independent gyroscopic survey after the well is drilled.

The Monte Carlo test draws realizations under the H_0 hypothesis. If the observed distance d^{obs} is too large compared with the realizations of distances under the hypothesis, we reject H_0. This rejection means 'no collision', i.e. the well plan is acknowledged and drilling can proceed. The p-value is calculated from the empirical percentile of the observed statistic under the simulated H_0 distribution. Again, if small p-values are noted at all stands of the well plan, the well plan is acknowledged.

A pseudoalgorithm for the Monte Carlo test is as follows:

1. Draw distances $d^1, \ldots, d^M$, under H_0, i.e. such that $|\boldsymbol{\mu}_q - \boldsymbol{\mu}_p| = \mu_{d,0}$.
2. Sort the distances under H_0 from smallest to largest to get $d^{(1)}, \ldots, d^{(M)}$.
3. Reject H_0 if $d^{\text{obs}} > d^{((1-\alpha)M)}$.
4. The p-value is the smallest η such that $d^{((1-\eta)M)} < d^{\text{obs}}$.

We use $M = 10000$ Monte Carlo runs to make the results below. The Monte Carlo error decreases with the number of samples, and can be made arbitrarily small by increasing M. Of course, the computation time also increases with M.

The simulation of distances in 1. above is carried out by first setting $\boldsymbol{\mu}_p = \hat{\boldsymbol{p}}$. Next, a three dimensional random vector $\boldsymbol{v}$ of length $\mu_{d,0}$ is generated and $\boldsymbol{\mu}_q = \boldsymbol{\mu}_p + \boldsymbol{v}$. Then drawing $\boldsymbol{p} \sim f(\boldsymbol{p})$ in equation (19) and drawing $\boldsymbol{q} \sim N(\boldsymbol{\mu}_q, \boldsymbol{\Sigma}_q)$. Finally, we set the distance $d = \sqrt{(\boldsymbol{p} - \boldsymbol{q})'(\boldsymbol{p} - \boldsymbol{q})}$.

Brought to you by | Universitetsbiblioteket I Trondheim NTNU Universitetsbiblioteket
Authenticated
Download Date | 10/7/19 3:25 PM

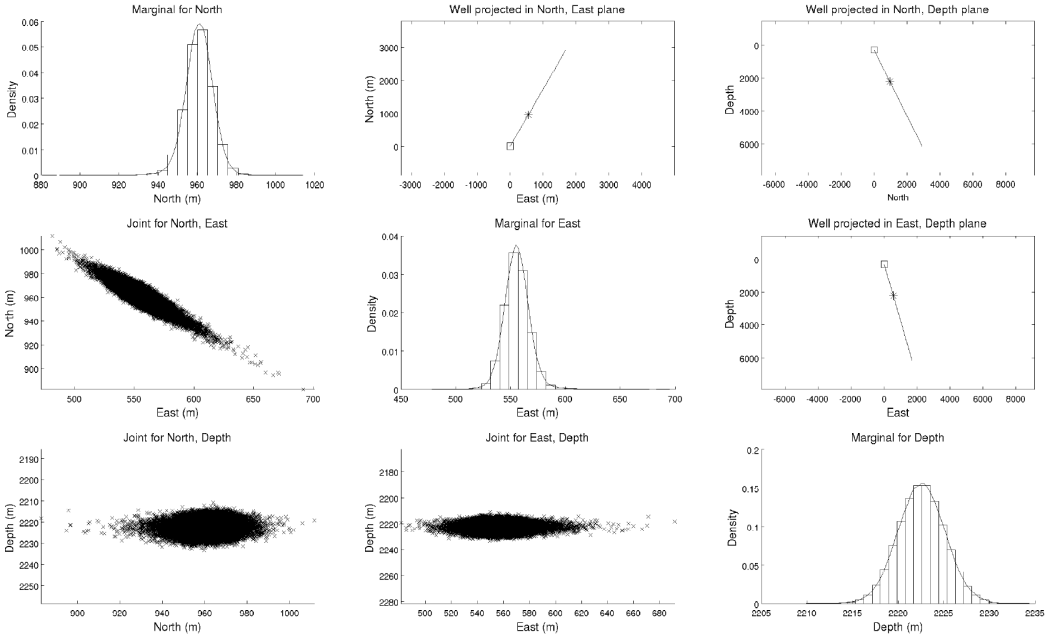

Figure 3. Well positioning distribution with NIG error source for magnetic declination angle. Diagonal entries represent marginals for north, east and vertical depth. Lower left displays are joint distributions for (north, east), (north, vertical) and (east, vertical). Upper right displays are well paths in north, east and vertical coordinates.

3. Results

We first present results for positioning using both normal and NIG distributions for magnetic reference errors. Next we compare the anti-collision calculations for NIG and normal with approximate and Monte Carlo test.

3.1. Position uncertainty

We illustrate the position of a straight well plan going in the north-east direction. This plan is shown to the upper right in Figure 3. We have tested various well geometries, and the uncertainty of the well position is very dependent on this geometry. Nevertheless, some general guidelines can be drawn from this simple example.

In Table 2 we show the position distribution percentiles for north, east and vertical depth coordinates in several cases. This table is representative for depth 2200 m. For the case in column one the normal distribution is used for all error sources, and the B_z component of the magnetometers is assumed reliable. The Earth's magnetic field strength and dip angle are not used in the error modeling. The case in column 2 also uses normal errors, but now the B_z component is not reliable, and thus the magnetic dip and field strength (also normally distributed in this case) are included in the model. The last two columns use NIG distributions for the magnetic reference values. We again study the case when the B_z component is available (one NIG error in column three) and when it is not trusted (three NIG errors in column four). The various versions of error modeling have no effect for the vertical depth. Differences between normal and NIG mean values for north and east coordinates appear to some extent for the ten percent lower and upper quantiles with a significant shift for the one percent lower and upper quantiles. The normal situation have smaller tails than the NIG case. When the B_z measurement is not used, the uncertainties in north and east increase slightly.

The lower left part of Figure 3 displays the position distributions in the same setting, obtained by using a NIG distribution for the magnetic declination angle. The marginal distributions for north, east and depth on the diagonal of this figure seem quite symmetric, but there is much probability mass in the tails. There is also some visible skewness in the plots. Note that the uncertainty seems to be largest orthogonal to the well path as a result of the physical relations for magnetic surveying.

3.2. Anti-collision

We compare the anti-collision calculations with one offset well and one reference well. For a proposed well plan we then compute the p-values of the hypothesis test described in Section 2.3. The offset well position is assumed normally distributed, while the reference well is assumed NIG or normally distributed. For the NIG case

VERSITA

Brought to you by | Universitetsbiblioteket I Trondheim NTNU Universitetsbiblioteket
Authenticated
Download Date | 10/7/19 3:25 PM

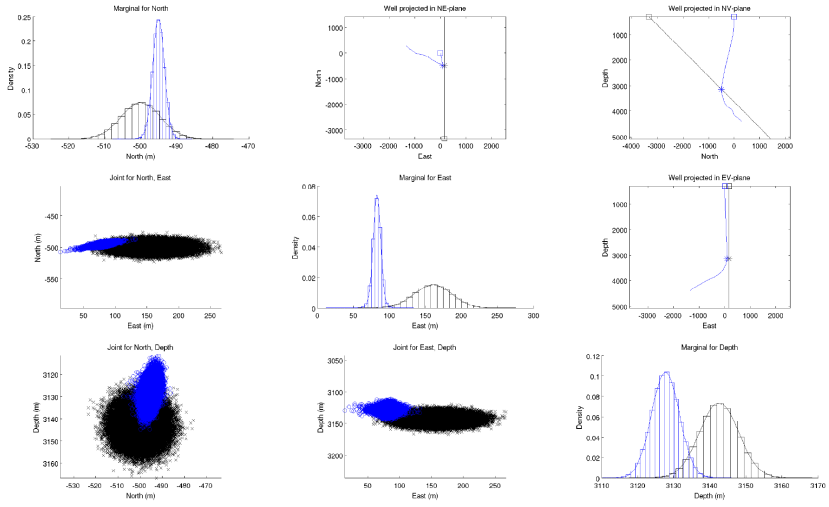

Figure 4. Well anti-collision case 1. Diagonal entries show the marginals for offset well (black) and reference well (blue). Lower left displays show joint distributions for (north, east), (north, depth) and (east, depth) for both offset well (black, crossed) and reference well (blue, circles). Upper right displays show the well paths for offset well (black) and reference well (blue) in north, east and vertical depth coordinates.

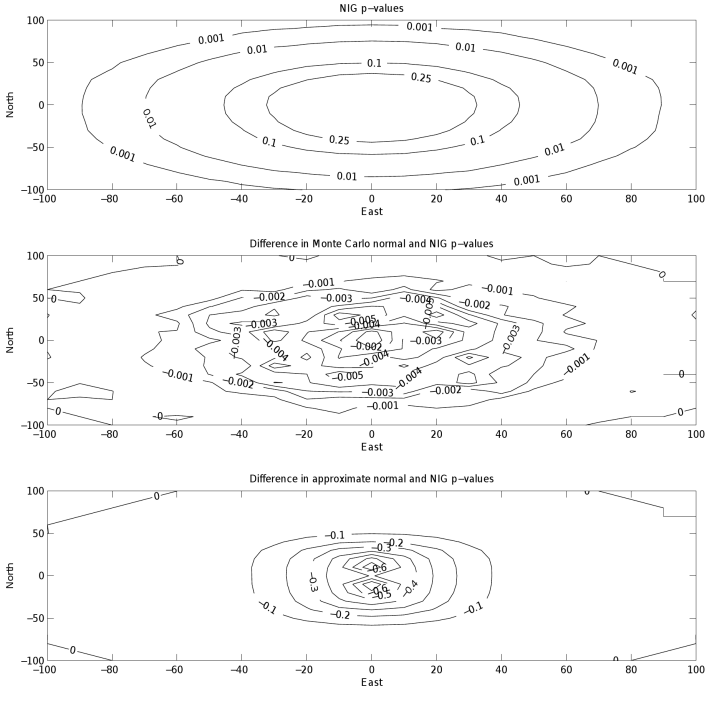

Figure 5. Well anti-collision case 1. Shifting the offset well on a grid of north, east coordinates. Top: p-values for the NIG model. Middle: p-value difference between NIG and normal case with Monte Carlo test. Bottom: p-value difference between NIG and normal case with approximate normal test.

VERSITA

Brought to you by | Universitetsbiblioteket I Trondheim NTNU Universitetsbiblioteket
Authenticated
Download Date | 10/7/19 3:25 PM

Table 2. Vertical depths near 2200 m: Well positioning distribution (in meters) represented by north, east and depth percentiles. Normal: All errors Gaussian. Normal (No B_z): all errors Gaussian, but magnetic dip and strength reference is used instead of B_z measurement. NIG: all errors Gaussian except magnetic declination reference which is NIG distributed. NIG (No B_z): all errors Gaussian except magnetic declination, dip and strength reference which are NIG distributed when the B_z is not available.

	Normal	Normal (No B_z)	NIG	NIG (No B_z)
N 1 %	948	947	943	942
N 10 %	954	954	952	952
N 50 %	961	961	961	961
N 90 %	969	969	970	970
N 99 %	975	975	977	978
E 1 %	534	533	529	527
E 10 %	543	543	542	541
E 50 %	555	555	555	555
E 90 %	567	567	570	570
E 99 %	577	577	586	587
D_V 1 %	2217	2217	2217	2217
D_V 10 %	2219	2219	2219	2219
D_V 50 %	2223	2223	2223	2223
D_V 90 %	2226	2226	2226	2226
D_V 99 %	2229	2229	2228	2228

we compute the p-value using Monte Carlo realizations. For the normal case we obtain the p-value by Monte Carlo realizations and by using the approximate normal test statistic.

Figure 4 illustrates a case with one straight offset well (black) and the planned deviated reference well (blue). The upper right part of Figure 4 shows estimated well position for offset well (black) and planned positions for the reference well (blue). The distribution for both wells at the stand with the shortest center-to-center distance (near 3000 m depth) is shown by the diagonal and lower left plots in Figure 4. Note that the reference well has shorter length at this stand, and its uncertainty is smaller. We assume that the B_z component is available, and the magnetic declination reference is the only NIG error component used for the reference well calculation.

For the well geometry shown in the upper right part in Figure 4 the NIG case has a p-value of 0.0030, the Monte Carlo normal p-value is 0.0027, while the p-value of the approximate normal test is 0.0013. This means that the approximate normal test has too small p-value. The NIG case and the Monte Carlo normal test have similar p-values, but the NIG case is slightly larger. This can be interpreted by studying the tails of the reference wells in the lower left plots in Figure 4 (blue). The chance of some very large distances is higher for the NIG model, and as a result the observed (planned) center-to-center distance is not so extreme for the NIG case.

We next compare anti-collision p-values for some different well geometries by shifting the offset well on a grid. The reference well remains at the same location as in Figure 4. The grid for the initial point for the offset well spans the shifts from -100 m to 100 m in north-south and east-west directions. In Figure 5 we plot p-values for NIG (top), differences between Monte Carlo normal and NIG (middle) and differences between approximate normal test and NIG (bottom). The top display in Figure 5 shows that the NIG model p-values decrease as we move the offset well away from the reference well. Note that the decay in p-value is not symmetric, since it decreases more rapidly in the east-west directions. This asymmetry represents the main uncertainty directions in the well positions, caused by the well geometry. In Figure 5 (middle) we see that the differences between p-values obtained for normal and NIG models are always negative, but they tend to zero when the center-to-center distance becomes large. The differences in Figure 5 (middle) are not very large, indicating that the use of a normal distribution instead of a NIG distribution for declination error does not have much influence on well planning for this kind of well geometry. We notice a certain pattern in Figure 5 in the sense that the largest differences occur in a circular domain about 25 m away from the origo. When comparing the NIG case with the normal case using an approximate normal test (Figure 5, bottom plot), we see that approximate normal p-values are far too small. The large differences indicate that the approximate test is not reliable, because it rejects the null hypothesis too often, and as a consequence approves well plans in high-risk situations. The figure shows a clear pattern, where the p-value differences tend to zero much faster for the east-west shifts than for the north-south shifts. This is caused by the well geometries and by the approximate test statistic.

In Figures 6 and 7 we show the result of anti-collision calculations for another situation with different well geometries. In this setting both offset and reference wells are drilled in the south-east direction and closer to the horizontal, as illustrated in Figure 6 (upper right). For this case no B_Z data is used, which entails three NIG error components; magnetic declination, dip and strength. The differences are then much larger between NIG and normal models. In Figure 6 the p-value for Monte Carlo normal is 0.04, while it is 0.08 for Monte Carlo NIG. Figure 7 shows the p-values obtained when shifting the offset well on a grid around the reference well. The pattern in the plots is the same as in Figure 5, but this time with larger differences between the NIG and normal Monte Carlo tests. For a distance of about 25 m the NIG p-value is about 0.05 larger (Figure 7 (middle plot)). This could have an impact on well planning decisions, since the hypothesis could be rejected for the normal model, and thus a high-risk well plan is approved. For the NIG model, one might accept the null hypothesis of a well collision, and thus decide to pursue another well path. The larger differences occur because of the new geometry of the well and the inclusion of the magnetic dip angle θ and field strength B in the azimuth calculations. Since the well is directed closer to the east horizontal, the weight functions for these error terms have a larger influence, and thus the NIG parameters are more dominant.

VERSITA

Brought to you by | Universitetsbiblioteket I Trondheim NTNU Universitetsbiblioteket
Authenticated
Download Date | 10/7/19 3:25 PM

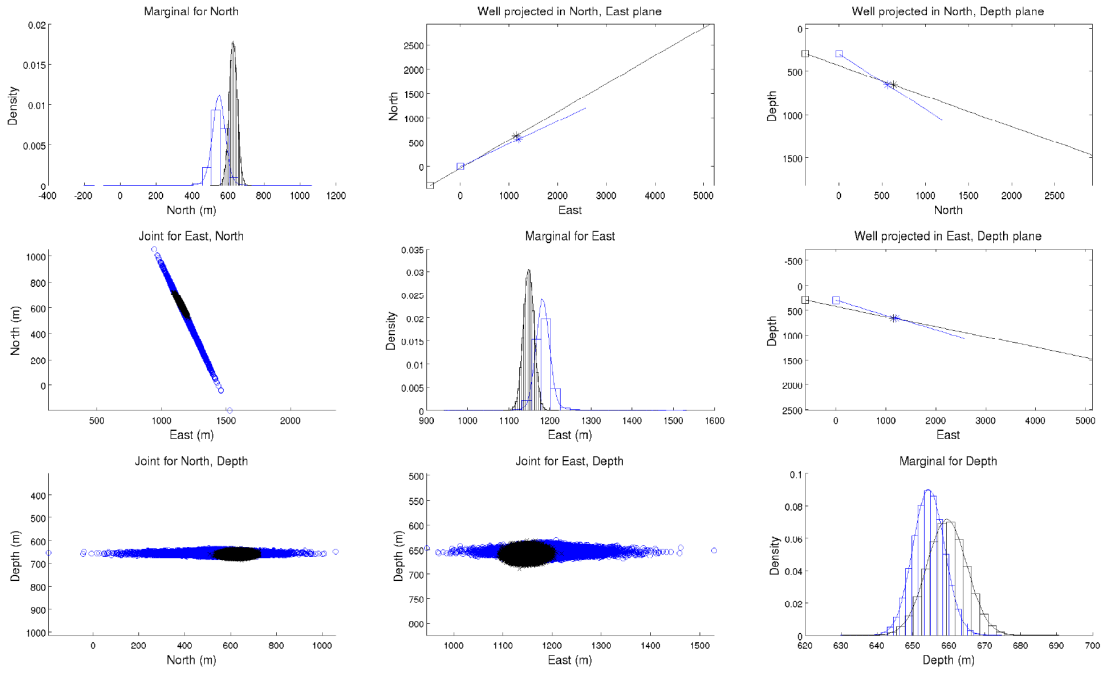

Figure 6. Well anti-collision case 2. Diagonal entries show the marginals for offset well (black) and reference well (blue). Lower left displays show joint distributions for (north, east), (north, depth) and (east, depth) for both offset well (black, crossed) and reference well (blue, circles). Upper right displays show the well paths for offset well (black) and reference well (blue) in north, east and vertical depth coordinates.

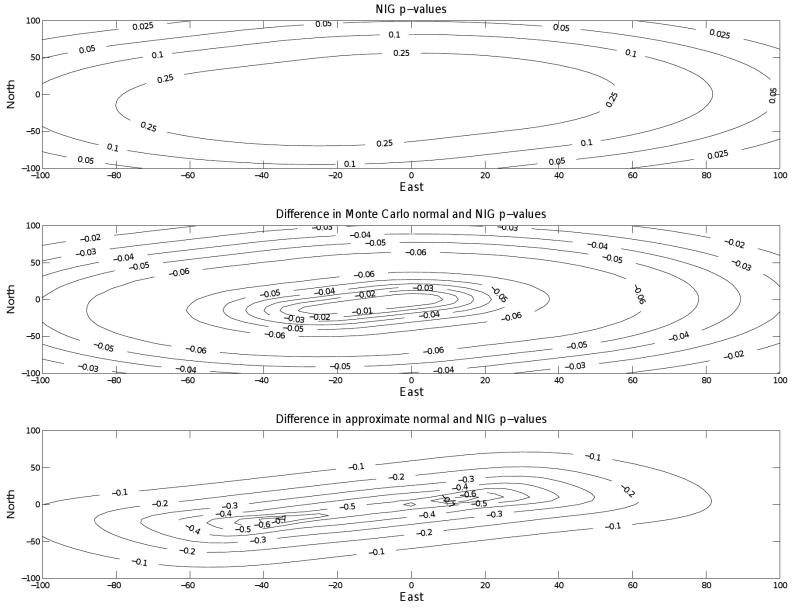

Figure 7. Well anti-collision case 2. Shifting the offset well on a grid of north, east coordinates. Top: p-values for the NIG model. Middle: p-value difference between NIG and normal case with Monte Carlo test. Bottom: p-value difference between NIG and normal case with approximate normal test.

VERSITA

Brought to you by | Universitetsbiblioteket I Trondheim NTNU Universitetsbiblioteket
Authenticated
Download Date | 10/7/19 3:25 PM

4. Discussion

In this paper we propose a new model for the positioning of wells in directional drilling, using heavy tailed NIG distributions for the magnetic reference values. This model captures the large variations in the Earth's magnetic field more accurately than the commonly used normal distribution. We use error propagation of the MWD magnetic directional drilling and the Earth's magnetic field reference errors to calculate the north, east and vertical depth position distribution.

The results are compared with the current state of the art based on the normal distribution for all error sources. The effect of including NIG error distributions depends on the well geometry. For the vertical depth coordinate we find no effects, while the east and north coordinates can be greatly affected when including the NIG terms.

For anti-collision calculations the effect of a NIG distribution again depends on the well geometry. We notice smaller p-values for the normal model than for the NIG model, and this indicates that a possibly high-risk well plan could be approved when using the normal model. The standard approach for anti-collision analysis is to use an approximate normal distributed test statistic to evaluate the significance of the center-to-center distance between two wells. Our experiments show that this approximate normal test is not reliable for small distances. It gives very small p-values compared with the normal Monte Carlo test. We recommend not using this approximate test for wells close to existing installations.

Acknowledgments

We thank Tromsø observational station for providing the magnetic measurement series, and Statoil for support.

References

Azzalini A., Capitanio A. (2003): Distributions generated by perturbation of symmetry with emphasis on a multivariate skew t-distribution. J. of the Royal Stat. Soc., Series B, 2003, 65, 367-389.

Bang J., Torkildsen T., Bruun B.T., Håvarstein S.T. (2009): Targeting challenges in Northern Areas due to the degradation of wellbore position accuracy. SPE/IADC Drilling conference and exhibition, SPE 119661-MS.

Barndorff-Nielsen O.E. (1997): Normal inverse Gaussian distributions and stochastic volatility modelling. Scand. J. Stat., 24, 1-13.

Ekseth R. (1998): Uncertainties in connection with the determination of wellbore positions. PhD thesis, Norwegian University of Science and Technoglogy, No. 1998:28.

Genton M.G. (2004): Skew-elliptical distributions and their applications: A journey beyond normality, Ed. Vol., Chapman& Hall.

Gjerde T. (2008): A heavy tailed statistical model applied in anti-collision calculations for petroleum wells. MSc thesis, Norwegian University of Science and Technoglogy.

Karlis D. (2000): An EM type algorithm for maximum likelihood estimation of the Normal Inverse Gaussian distribution. Stat and Prob letters, 57, 43-52.

Merrill R.T. (1983): The Earth's magnetic field, Academic Press.

Noureldin A., Irvine-Halliday D., Mintchev M.P. (2004): Measurement-while-drilling surveying of highly inclined and horizontal well sections utilizing single axis gyro sensing system. Measurement Sci and Tech, 15, 2426-2434.

Nyrnes E. (2006): Error analyses and quality control of wellbore directional surveys. PhD thesis, Norwegian University of Science and Technoglogy, No. 2006:135.

Rector J.W., Marion B.P. (1991): The use of drill-bit energy as a downhole seismic source. Geophysics, 56, 628-634.

Skarsbø E., Ernesti K.D. (2006): Geosteering precisely places multilaterals in NorwayâĂŹs Troll field. Oil & gas journal, 104, 49-62.

Thorogood J.L., Sawaryn S.J. (2005): A compendium of directional calculations based on the minimum curvature method. SPE Drilling and completion, 20, 24-36.

Tukey J.W. (1960): A survey of sampling from contaminated distributions. Contributions to Probability and Statistics, I. Olkin (ed.), Stanford, CA: Stanford University Press.

Williamson H.S. (1998): Towards risk-based well separation rules. SPE Drilling and completion, 13, 47-51.

Williamson H.S. (2000): Accuracy prediction for directional measurement while drilling. SPE Drilling and completion, 15, 221-233.

Wolff CJM, de Wardt JP (1981): Borehole position uncertainty - analysis of measuring methods and derivation of systematic error model. Journal of Petr Tech, 33:2339-2350.

Øigård T.A., Hanssen A., Hansen R.E., Godtliebsen F. (2005): EM-estimation and modeling of heavytailed processes with the multivariate normal inverse Gaussian distribution. Signal Proc, 85, 1655-1673.

Brought to you by | Universitetsbiblioteket I Trondheim NTNU Universitetsbiblioteket
Authenticated
Download Date | 10/7/19 3:25 PM